ISBN: 978-3-95450-240-0 ISSN: 2673-5547 doi:10.18429/JACoW-HIAT2022-TU1C4

A 3D PRINTED IH-TYPE LINAC STRUCTURE – PROOF-OF-CONCEPT FOR ADDITIVE MANUFACTURING OF LINAC RF CAVITIES*

H. Hähnel†, A. Ateş, U. Ratzinger
Institute of Applied Physics, Goethe University, Frankfurt a. M., Germany

Abstract

Additive manufacturing (AM or "3D printing") has become a powerful tool for rapid prototyping and manufacturing of complex geometries. A 433 MHz IH-DTL cavity has been constructed to act as a proof of concept for additive manufacturing of linac components. In this case, the internal drift tube structure has been produced from 1.4404 stainless steel using 3D printing. We present the concept of the cavity as well as first results of vacuum testing and materials testing. Vacuum levels sufficient for linac operation have recently been reached with the AM linac structure.

INTRODUCTION

Additive manufacturing (AM) of metal parts may provide an interesting new way to manufacture accelerator components. As technology is evolving, the quality and accuracy of parts manufactured this way is improving. Recently, a number of studies on the topic of AM for linear accelerator components have been published [1–5]. Based on these promising results, we aim to evaluate the suitability of AM parts for direct manufacturing of normal conducting linac structures. To that end, a reproduction of the beam pipe vacuum tests in [2, 3] was performed and upon success, a prototype cavity with a fully printed drift tube structure was constructed. The cavity is designed to be UHV capable and includes cooling channels reaching into the stems of the drift tube structure for power testing with a pulsed 30 kW rf amplifier.

Prototype Design and Concept

The prototype cavity was designed for a resonance frequency of 433.632 MHz, which is a harmonic of the GSI UNILAC operation frequency [6]. In combination with a targeted proton beam energy of 1.4 MeV this scenario allows for a compact accelerator at the limits of feasibility and is therefore a good benchmark for the new approach. The internal drift tube structure is fully 3D printed from stainless steel (1.4404), see Fig. 1a. Due to the lower complexity of the cavity frame and lids, they are manufactured by CNC milling of bulk stainless steel. Printing those parts would not be cost efficient.

The cavity is just 22 cm wide and 26 cm high (outer walls), with a length of 20 cm on the beamline (flange to flange). A center frame acts as the foundation for the cavity. This 7 cm high center frame provides the precision mount points for the girder-drift tube structures and end-drift tubes. While the end-drift tubes are mounted in vacuum, the girders have a vacuum sealing surface at the bottom. Two half shells are mounted on the top and bottom of the center frame. The cavity is equipped with four CF40-Flanges for vacuum, rf-coupler and tuner, as well as metal sealed KF40 flanges for the beamline and smaller ports for diagnostics. Rf simulations show that the bulk of the rf losses during the operation of this cavity is concentrated on the drift tube structure and the cavity frame. Therefore, water channels are included in the girders up to the drift tubes and also in the center frame. A 3D CAD view of the full construction is shown in Fig. 1b.

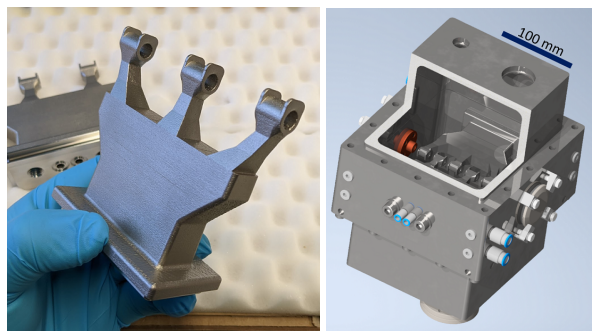

(a) (b)

Figure 1: Overview of the cavity geometry and printed parts. (**a**) 3D printed girder drift tube structure. (**b**) Cross section of the assembled cavity model.

RF Simulations

The cavity design was optimized for a frequency of 433.632 MHz. To minimize the need for support structures during the manufacturing process, the shape of the girder-drift tube structure was optimized to reduce overhang. Simulations of electromagnetic fields in the cavity were performed with the CST Microwave Studio eigenmode solver. Figure 2 shows the resulting electric field distribution in the cavity, with the typical characteristics of a $\beta\lambda/2$ IH-type structure. From the idealized design model, the simulated dissipated power for the effective acceleration voltage of U_{eff} = 1 MV is P_{loss} = 24.82 kW. With an inner wall length of 146 mm, this corresponds to an effective shunt impedance of Z_{eff} = 287.13 MΩ/m[1], showing the high efficiency of such an IH-type structure.

EXPERIMENTS

Since the first construction of the cavity in late 2020/early 2021, several experiments have been conducted to evaluate certain aspects of the cavity suitability for linac operation. The following sections will explore the different experiments.

* Work supported by BMBF 05P21RFRB2
† haehnel@iap.uni-frankfurt.de

[1] The stated value in [7] was much too low, due to a typo.

ISBN: 978-3-95450-240-0 ISSN: 2673-5547 doi:10.18429/JACoW-HIAT2022-TU1C4

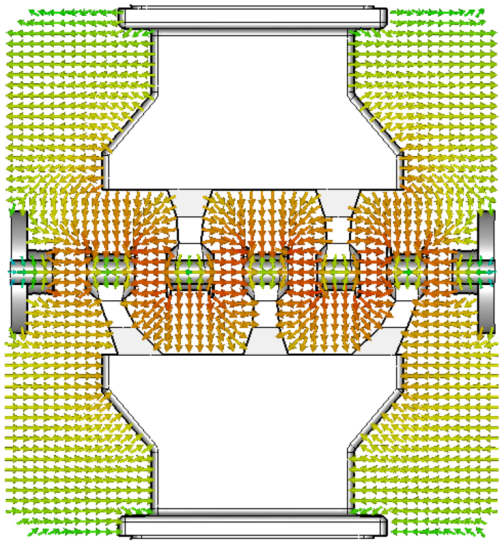

Figure 2: Electric field distribution in the prototype cavity.

Water Flow Measurements

Both girder-drift tube structures, as well as the center frame of the cavity are water cooled. While the water cooling in the center frame is quite conventional and realized with deep-hole drilled channels, the water cooling in the girders is more complex. To ensure, that the water channels in the girders are working as intended and not blocked by, for example, residual metal powder, some flow measurements were performed. The setup is provided with a water pressure of 8 bar. The tubing used is Festo tubing with an outer diameter of 6 mm. Measurements were performed with a Kobold digital inductive flow meter. Measurement results are summarized in Table 1.

Table 1: Waterflow Measurement

Scenario	Water Flow
Source	10.8 L/min
6 mm tubing	7.2 L/min
Girder 1	4.8 L/min
Girder 2	5 L/min
Girder 1&2 parallel	7.6 L/min

As expected, the complex inner structure of the cooling channels leads to a reduction in flow. However, the measurements show that significant cooling can be expected for these structures.

Preliminary Vacuum Tests

To evaluate the performance of 3D printed components in a UHV environment, preliminary tests were performed with 3D printed beam pipes with KF40 flanges (see Fig. 3). These pipes were printed in 1.4404 stainless steel and the sealing surfaces on both ends were turned down on a lathe at the IAP workshop to provide a good vacuum seal. The inside and outside surfaces of the pipes were left as manufactured. A commercially available conventionally manufactured beam pipe of identical dimensions was acquired from Pfeiffer Vacuum for comparison. Both the printed and the conventional pipes were then connected to a small 18 L/s turbomolecular pump and repeatedly evacuated and flushed with nitrogen gas.

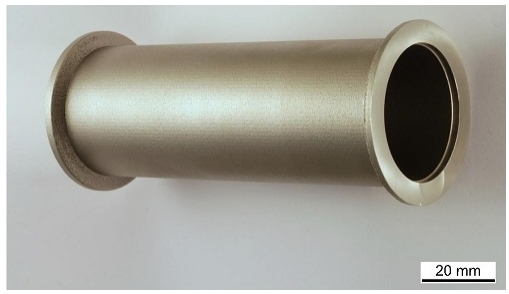

Figure 3: KF 40 pipe printed from stainless steel.

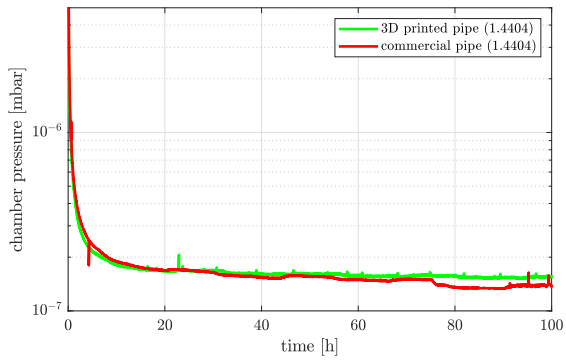

Figure 4: Pumpdown curve of the fourth vacuum cycle of the KF40 test pipes.

Since these pipes were not cleaned and were used as manufactured, some initial outgassing was expected. The experiment showed some interesting results. For one, as expected with each pumping and flushing cycle, the pump down time to a certain pressure point was taking less time with each iteration. Also, it seems, that the rough surface on the inner wall of the printed pipe does not pose a big problem. In the end, both pipes performed very similar and the pumping curve as well as the achieved final pressure were indistinguishable within the accuracy limitations of the experiment. Pressure data of the fourth pumping cycle are shown in Fig. 4.

The final pressure achieved was about 2×10^{-7} mbar for both the conventional and the printed pipe. Similarly promising results were reported in, for example, [3,4]. These results certainly show promise for the UHV capability of printed parts.

Printed Material Properties

To assess the material properties, one of the printed stainless steel pipes was sent to a materials testing lab. Surface roughness was found to be in the order of R_z = 16.05–37.52 µm dependent on location and orientation of the measurement. Material porosity was determined to be 0.04 % by optical analysis of material cross-sections (see e.g., Fig. 5a,c). Larger cavities in the material were found on the outside of the flange, especially in the areas, where the flange extends outward from the pipe. The pipe was printed standing

ISBN: 978-3-95450-240-0 ISSN: 2673-5547 doi:10.18429/JACoW-HIAT2022-TU1C4

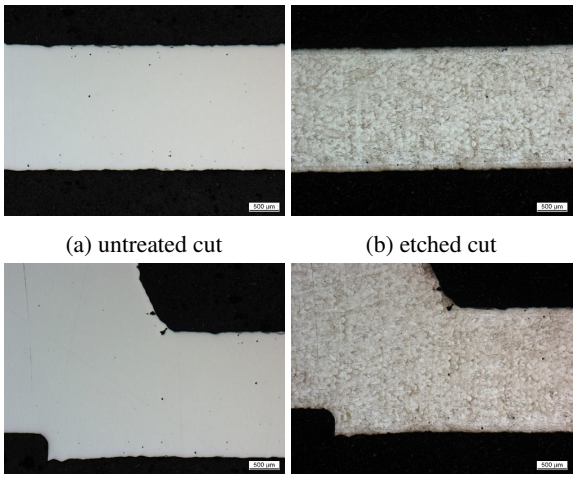

(a) untreated cut (b) etched cut

(c) untreated cut (d) etched cut

Figure 5: Prepared cross sections of printed KF40 pipe wall material (bright areas = steel). The top images show a cross-section of the pipe wall, the bottom images show the region around the KF 40 flange. Courtesy of GSI Darmstadt, pLinac project.

upright and therefore this area was not supported by bulk material during the printing process. Within the bulk material of the pipe, no large cavities were found. The melt-pool structure of the bulk material, which is caused by the manufacturing process, can be seen in the etched cross-sections in Fig. 5b,d. Overall, the material seems well suited for vacuum applications as the degree of the porosity is not concerning. Depending on the application, further surface treatment will be necessary to reduce surface roughness.

Polishing and Copper Plating

The initial batch of AM IH-structures has been polished in a slide grinding machine. The results are promising, however for the current geometry there are some areas that cannot be reached by the granule particles as well as the flat sides. Consequently, a new geometry is currently being designed to mitigate these issues. Following the surface polishing, the structures have been copper plated with an approximate layer thickness of 50 µm. Optical inspection shows a very clean result of the copper plating (see Fig. 6). Vacuum and rf tests with the copper plated components are planned to assess the quality of the copper layer.

FULL CAVITY VACUUM TESTS

The cavity was fully assembled in early May 2021 (see Fig. 7). For first vacuum tests, the cavity was attached to a turbo-molecular pump (Pfeiffer HiPace80) via one of the top CF40 flanges. A vacuum gauge (Pfeiffer PKR261) was used to measure and log the cavity vacuum. The cavity lids, as well as the girder drift tube structures were sealed using 1.5 mm aluminum wire. Following the publication of [7], where a chamber pressure of 1.19×10^{-6} mbar was reached, the cavity was disassembled and some revisions to sealing surfaces, as well as additional provisions for a dedicated pre-vacuum system were made.

New Vacuum measurements were performed in early 2022 and a pressure of 1.4×10^{-7} mbar was reached. This demonstrates, that even direct vacuum sealing surfaces can be manufactured with 3D printing. Of course, the surface has to be milled flat after printing, as the surface roughness of a raw printed part would not suffice. At this vacuum level, high power rf experiments are possible. Further improvements of the vacuum are expected from heat treatment to speed up outgassing. This pump-down curve from the latest measurement is shown in Fig. 8.

LOW-LEVEL RF TESTS

Low-level rf measurements were performed with a network analyzer to confirm the frequency and Q-factor of the cavity without any copper plating. For comparison, CST simulations were performed with the final design CAD geometry of the components, to get as close to the manufactured cavity as possible. Simulations were performed with an electrical conductivity of $\sigma_{Cu} = 5.8 \times 10^7$ S/m and $\sigma_{1.4404} = 1.3 \times 10^6$ S/m for copper and stainless steel respectively. Table 2 compares the simulation results with the performed measurements. At critical coupling, the measured resonance frequency is only 79 kHz higher than simulated. The measured unloaded quality factor of the cavity $Q_0 = 1132$ is also reasonably close to the simulated value of $Q_0 = 1321$ for stainless steel. Calculating the quality factor for stainless steel relies on the actual conductivity value of the steel used during manufacturing an can therefore only be approximated based on spec-sheets.

Table 2: Comparison of rf simulation and measurement

Parameter	Simulation	Measurement
f_{res}	433.445 MHz	433.524 MHz
Q_0 (steel)	1321	1132
Q_0 (copper)	8715	-
Z_{eff} (copper)	241.2 MΩ/m	-

CONCLUSION

Most recent vacuum tests showed, that a cavity pressure of 1.4×10^{-7} mbar could be reached without issue. First low-level rf measurements confirmed the operating frequency and also showed good agreement for the stainless-steel Q-factor of the cavity. Overall, the current results show promise for the reality of 3D printed linacs in the near future. The project aims to further investigate the pros and cons of this technology.

NEXT STEPS

Next up are low-level rf measurements with the printed copper plated IH-structures. After these measurements, the cavity lids and center frames will also be copper plated soon. Finally, the structure will be tested at full power with a 30 kW pulsed rf amplifier.

ISBN: 978-3-95450-240-0 ISSN: 2673-5547 doi:10.18429/JACoW-HIAT2022-TU1C4

Figure 6: First iteration of AM stainless-steel IH-structures after polishing and galvanic copper-plating.

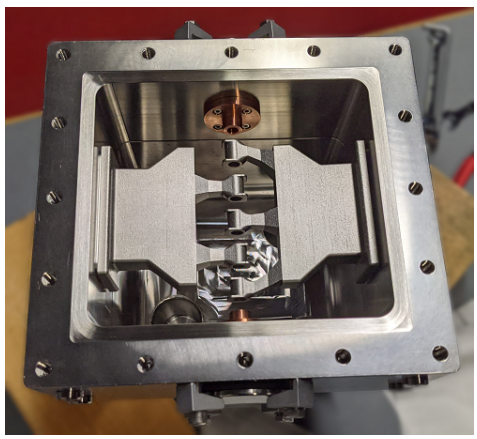

Figure 7: Top view of the cavity during first assembly with installed drift tube structure.

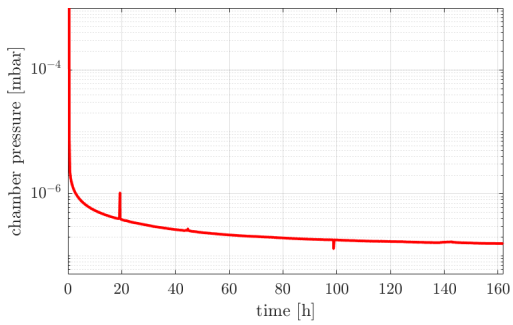

Figure 8: Pumpdown curve of the fully assembled cavity after revision and reassembly in 2022. Peak at 20 h corresponds to opening of the dedicated pre-vacuum valve.

Girder Design Improvements

A first design improvement was done in late 2021 by the inclusion of a dedicated pre-vacuum system. Currently, the overall shape of the girder-drift tube structures is being improved to achieve several goals:

- improved printing performance,
- improved polishing results,
- rf performance improvements.

A first draft of this improved geometry is shown in Fig. 9. The smooth transitions improve the polishing performance, as well as reduce peak fields during copper plating and operation. A set of the improved structures will be printed soon.

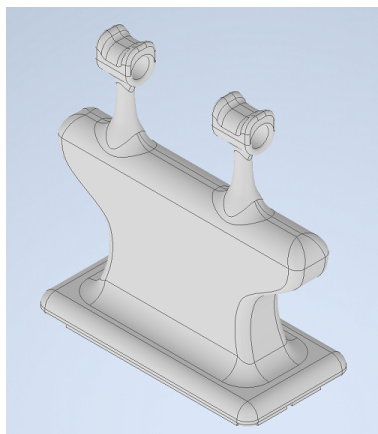

Figure 9: Improved geometry for the AM IH-structure.

ACKNOWLEDGEMENTS

The authors would like to acknowledge the contribution of material analysis of printed parts, which was organized and funded by the GSI Darmstadt proton linac project team.

REFERENCES

[1] P. Frigola *et al.*, "Advance Additive Manufacturing Method for SRF Cavities of Various Geometries", in *Proc. SRF'15*, Whistler, Canada, Sep. 2015, pp. 1181–1184. doi:10.18429/JACoW-SRF2015-THPB042

[2] S. Jenzer *et al.*, "Study of the Suitability of 3D Printing for Ultra-High Vacuum Applications", in *Proc. IPAC'17*, Copenhagen, Denmark, May 2017, pp. 3356–3358. doi:10.18429/JACoW-IPAC2017-WEPVA043

[3] G. Sattonnay *et al.*, "Is it Possible to Use Additive Manufacturing for Accelerator UHV Beam Pipes?", in *Proc. IPAC'19*, Melbourne, Australia, May 2019, pp. 2240–2243. doi:10.18429/JACoW-IPAC2019-WEXXPLS3

[4] C. R. Wolf, F. B. Beck, L. Franz, and V. M. Neumaier, "3D Printing for High Vacuum Applications", in *Proc. Cyclotrons'19*, Cape Town, South Africa, Sep. 2019, pp. 317–320. doi:10.18429/JACoW-CYCLOTRONS2019-THC04

[5] N. Delerue *et al.*, "Prospects of Additive Manufacturing for Accelerators", in *Proc. IPAC'19*, Melbourne, Australia, May 2019, pp. 4118–4120. doi:10.18429/JACoW-IPAC2019-THPTS008

ISBN: 978-3-95450-240-0 ISSN: 2673-5547 doi:10.18429/JACoW-HIAT2022-TU1C4

[6] U. Ratzinger, "The New High Current Ion Accelerator at GSI and Perspectives for Linac Design Based on H-Mode Cavities", in *Proc. EPAC'00*, Vienna, Austria, Jun. 2000, paper TUZF204, pp. 98-102.

[7] H. Hähnel, U. Ratzinger, "First 3D Printed IH-Type Linac Structure – Proof-of-Concept for Additive Manufacturing of Linac RF Cavities", in *Instruments*, vol. 6, no. 1, p. 9, 2022. doi:10.3390/instruments6010009